On the Use of the Hypothesis of Local Electroneutrality in Colloidal Suspensions for the Calculation of Their Dielectric Properties

J. J. López-García,[†] C. Grosse,[‡,§] and J. Horno*[,†]

Departamento de Física, Campus Las Lagunillas, Ed. A3, Universidad de Jaén, 23071, Jaén, Spain, Departamento de Física, Universidad Nacional de Tucumán, San Miguel de Tucumán, Argentina, and Consejo Nacional de Investigaciones Científicas y Técnicas, Buenos Aires, Argentina

Received: November 29, 2004; In Final Form: January 26, 2005

The validity of the hypothesis of electroneutrality outside the double layer of a suspended particle with an applied ac electric field is analyzed. It is shown that the electrolyte solution remains electroneutral for distances greater than a few Debye lengths from the particle surface only when the diffusion coefficients of the two ion species are identical. On the contrary, in the general case, a volume charge density around the particle builds up, which extends to distances that are proportional to the square root of the effective diffusion coefficient value divided by the frequency. These distances can easily attain many particle radii. Numerical results for both uncharged and charged suspended particles are presented, and a correction to existing analytical expressions for the field-induced ion distributions around uncharged particles (*J. Phys. Chem.* **2004**, *108*, 8397) is given. While the charge densities far from the particle are usually very weak, it is shown that they strongly contribute to the dipole coefficient value and, therefore, to the calculated values of the permittivity and conductivity increments. The errors that would be committed if these charge densities were ignored, assuming local electroneutrality and determining the dipole coefficient at a few Debye lengths from the particle surface, are analyzed and shown to be substantial.

Introduction

It is well-known that, due to the presence of the particles, the complex permittivity $\epsilon^*(\omega)$ of a suspension differs from that of the supporting electrolyte solution $\epsilon_e^*(\omega)$.[1,2] For dilute suspensions:

$$\epsilon^*(\omega) = \epsilon_e^*(\omega) + p\Delta\epsilon^*(\omega) \tag{1}$$

where p is the volume fraction of solids, ω is the angular frequency and $\Delta\epsilon^*(\omega)$ is the complex permittivity increment. This last magnitude mainly depends on the zeta potential of the particles, ζ, on the conductivity of the electrolyte solution:

$$k_e = \frac{Nz^+ z^- e^2(z^+ D^+ + z^- D^-)}{kT} \tag{2}$$

and on the product κR, where κ is the reciprocal Debye length,

$$\kappa = \sqrt{\frac{z^+ z^- (z^+ + z^-)e^2 N}{kT\epsilon_e}} \tag{3}$$

and R is the particle radius. In these expressions $z^{\pm}$ are the unsigned valences of the two ionic species in the electrolyte solution, $D^{\mp}$ are their diffusion coefficients and $z^- N$ their number concentrations (ions per unit volume) far from any particle. On the other hand, k is the Boltzmann constant, T the absolute temperature, e the elementary charge, and ϵ_e the absolute permittivity of the electrolyte solution.

Equation 1 makes it possible to calculate the permittivity and conductivity increments:[1]

$$\Delta\epsilon(\omega) = 3\epsilon_e\left[K_d'(\omega) + \frac{k_e}{\omega\epsilon_e}K_d''(\omega)\right] \tag{4}$$

$$\Delta k(\omega) = 3k_e\left[K_d'(\omega) - \frac{\omega\epsilon_e}{k_e}K_d''(\omega)\right] \tag{5}$$

where $K_d = K_d' + iK_d''$ is the complex induced dipole coefficient of the particle. To calculate this coefficient, the coupled equation system made of the Nernst−Planck, Poisson, and Navier−Stokes equations, needs to be solved in the region outside the particle. Since this is in general very complicated, because of the triple origin (convective, diffusive, and electrical) of the ionic transport in the suspension, a number of methods have been devised in order to obtain either approximate[1,3−6] or numerical solutions.[7−9] In all the numerical works, the induced dipole coefficient K_d is calculated assuming that outside the electrical double layer there is local electroneutrality

$$z^+ \delta C^+ - z^- \delta C^- = 0 \tag{6}$$

where $\delta C^{\pm}$ are the ion concentration changes induced by the applied field $\vec{E}$. Under this assumption, the electric potential $\Phi(\vec{r},\omega)$ takes the following form:

$$\Phi(\vec{r},\omega)|_{r\to\infty} = -\vec{E}\cdot\vec{r} + K_d(\omega)R^3\frac{\vec{E}\cdot\vec{r}}{r^3} \tag{7}$$

Therefore, if the value of the electric potential at a point outside the double layer is known, expression 7 permits one to easily calculate the induced dipole coefficient.

* Corresponding author.
[†] Universidad de Jaén.
[‡] Universidad Nacional de Tucumán.
[§] Consejo Nacional de Investigaciones Científicas y Técnicas.

10.1021/jp044585l CCC: $30.25
Published on Web 03/03/2005

However, condition 6 is not required in analytical calculations,[1,6] which only use the hypothesis of an approximate local electroneutrality: the sum of the low-frequency field-induced changes of the counterion and co-ion densities outside the double layer is much greater than their difference.

In most of the literature, it is accepted that the thickness of the electric double layer is of the order of a few Debye lengths. Therefore, for greater distances to the particle surface, the electroneutrality condition is fulfilled and expressions 6 and 7 can be used to calculate the permittivity and conductivity increments. In what follows we shall show that while, as is usually accepted, electroneutrality in the solution is reached at a few Debye lengths from the particle surface both for dc and ac electric fields when the diffusion coefficients of the two ionic species are identical, the situation drastically changes when these diffusion coefficients differ from one another. Under these more general conditions, the distance to the particle surface of the spatial points at which eq 7 is valid is given by the characteristic diffusion lengths of the ions. This fact should be taken into account in order to avoid substantial errors in the evaluation of the permittivity and conductivity increments.

Theory

Basic Equations. We consider a nonconducting spherical particle with absolute permittivity ϵ_i, immersed in an electrolyte solution with viscosity η. The equations governing the dynamics of the system are well-known:[1-2]

(i) Nernst−Planck equations for the ionic flows:

$$\vec{j}^{\pm}(\vec{r},t) = -D^{\pm}\nabla C^{\pm}(\vec{r},t) \mp \frac{z^{\pm}eD^{\pm}}{kT}C^{\pm}(\vec{r},t)\nabla\Phi(\vec{r},t) + C^{\pm}(\vec{r},t)\vec{v}(\vec{r},t) \quad (8)$$

(ii) Conservation equation for each ionic species:

$$\nabla\cdot\vec{j}^{\pm}(\vec{r},t) = -\frac{\partial C^{\pm}(\vec{r},t)}{\partial t} \quad (9)$$

(iii) Poisson equation:

$$\nabla^2\Phi(\vec{r},t) = -\frac{e[z^+C^+(\vec{r},t) - z^-C^-(\vec{r},t)]}{\epsilon_e} \quad (10)$$

(iv) Continuity equation for an incompressible fluid:

$$\nabla\cdot\vec{v}(\vec{r},t) = 0 \quad (11)$$

(v) Navier−Stokes equation for a viscous fluid:

$$\eta\nabla^2\vec{v}(\vec{r},t) - \nabla P(\vec{r},t) = e[z^+C^+(\vec{r},t) - z^-C^-(\vec{r},t)]\nabla\Phi(\vec{r},t) + \rho_f\left\{[\vec{v}(\vec{r},t)\cdot\nabla]\vec{v}(\vec{r},t) + \frac{\partial\vec{v}(\vec{r},t)}{\partial t}\right\} \quad (12)$$

where $\vec{j}^{\pm}$ is the local ionic flux (ions per unit area and time), $\vec{v}$ is the velocity field of the suspending medium, P is the pressure, t the time variable, and ρ_f the mass density of the suspending medium.

Equilibrium Situation. Without an applied electric field there are no net forces acting on the particles and ions in the system, so that $\vec{v}(\vec{r})$ and $\vec{j}^{\pm}(\vec{r})$ are all equal to zero. In this case, eq 8 can be solved and the results combined with eq 10 leading to the Poisson−Boltzmann equation:

$$\nabla^2\tilde{\Phi}_0(r) = -\kappa^2\frac{\exp[-z^+\tilde{\Phi}_0(r)] - \exp[+z^-\tilde{\Phi}_0(r)]}{z^+ + z^-} \quad (13)$$

Here

$$\tilde{\Phi}_0(r) = \frac{e\Phi_0(r)}{kT} \quad (14)$$

is the dimensionless potential and the lower index "0" denotes that there is no applied electric field; i.e., the system is in equilibrium.

Solutions for this equation have been given in numerous works,[10-14] where it is demonstrated that the thickness of the equilibrium electric double layer of the order of a few Debye lengths. This is illustrated in Figure 1 where the charge density profiles (normalized to their value at the particle surface) are represented for a ζ potential of 100 mV, $R = 100$ nm, and the indicated κ^{-1} values. These last values have also been plotted by means of vertical lines for comparison. The different curves show that, in all cases, the Debye length is a good approximation of the equilibrium electric double layer thickness: further than a few Debye lengths from the surface of the particle the system is locally electroneutral. Besides, these results are independent of the ion diffusion coefficient values, as expected, due to the independence of the Poisson−Boltzmann eq 13 on these parameters.

Nonequilibrium Situation. When an external field $\vec{E}(t)$ is applied to the system, all scalar variables are perturbed around their equilibrium values:

$$C^{\pm}(\vec{r},t) = C_0^{\pm}(r) + \delta C^{\pm}(r,t)\cos\theta \quad (15)$$

$$\Phi(\vec{r},t) = \Phi_0(r) + \delta\Phi(r,t)\cos\theta \quad (16)$$

These expressions were written using the usual assumption that the applied field is sufficiently weak so that all the perturbation terms are linear in E, and considering a reference frame, centered on the particle, with polar axis in the direction of $\vec{E}$. The vector quantities of the problem are also linear in E and can be written as

$$\vec{j}^{\pm}(\vec{r},t) = j_r^{\pm}(r,t)\cos\theta\hat{e}_r + j_\theta^{\pm}(r,t)\sin\theta\hat{e}_\theta \quad (17)$$

$$\vec{v}(\vec{r},t) = v_r(r)\cos\theta\hat{e}_r + v_\theta(r)\sin\theta\hat{e}_\theta \quad (18)$$

where $\hat{e}_r$ and $\hat{e}_\theta$ are the unit vectors in spherical coordinates.

Substituting expressions 15−18 into the basic equations 8−12 and neglecting second and higher orders terms in the perturbations, leads to the equation system that is actually solved. The boundary conditions for this problem have been widely described,[1-2] so only a brief account will be given here.

Conditions far from the particle:

$$\left.\frac{\partial\delta\Phi(r,t)}{\partial r}\right|_{r\to\infty} \to -E(t) \quad (19)$$

$$v_r(r\to\infty,t) \to -v_p(t) \quad (20)$$

$$\delta C^{\pm}(r\to\infty,t) \to 0 \quad (21)$$

$$\Omega(r\to\infty,t) \to 0 \quad (22)$$

where $v_p(t)$ is the electrophoretic velocity of the particle and $\vec{\Omega}(r,t)$ is the vorticity of the fluid defined as

$$\vec{\Omega}(r,t) = \nabla\times\vec{v}(r,t) \quad (23)$$

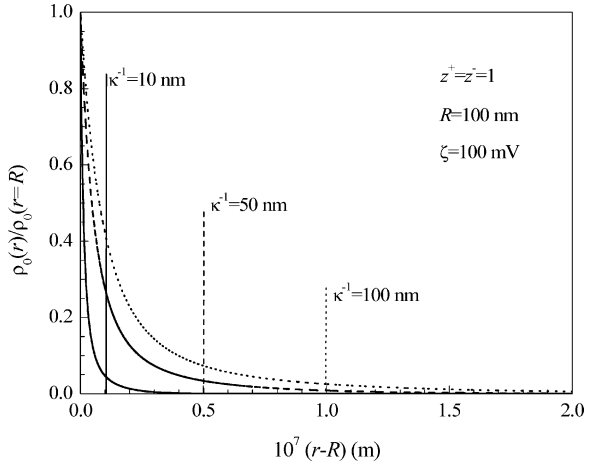

Figure 1. Equilibrium charge density profiles for the indicated κ^{-1} values, univalent ions, $R = 100$ nm, $\zeta = 100$ mV.

Conditions at the particle surface are as follows.

Continuity of the electric potential and of the normal component of the displacement vector:

$$\left.\frac{\partial \delta\Phi(r,t)}{\partial r}\right|_{r=R} = \frac{\epsilon_i}{\epsilon_e}\frac{\delta\Phi(r=R,t)}{R} \tag{24}$$

Adhesion condition for the radial component of the fluid velocity:

$$v_r(r=R,t) = 0 \tag{25}$$

Adhesion condition for the tangential component of the fluid velocity combined with the incompressibility equation:

$$\left.\frac{\partial v_r(r,t)}{\partial r}\right|_{r=R} = 0 \tag{26}$$

Impenetrability for all the ion types combined with the Nernst−Planck equation and eq 25:

$$\left.\frac{\partial}{\partial r}\left[\frac{\delta C^{\pm}(r,t)}{C_0{}^{\pm}(r)} \mp \frac{z^{\pm}e\delta\Phi(r,t)}{kT}\right]\right|_{r=R} = 0 \tag{27}$$

Equation of motion for the suspended particle:

$$F_e + F_m = -m_p\frac{\partial v_r(r\to\infty,t)}{\partial t} \tag{28}$$

where m_p is the mass of the particle while $\vec{F}_e$ and $\vec{F}_m$ are the electrical and mechanical forces acting on the particle.

Numerical Calculations. Numerical calculations for the solution of this system are somewhat more involved than in the case of the Poisson−Boltzmann equation. In this paper, we use the network simulation method, which consists of modeling the governing differential equations by means of an electrical circuit that is analyzed using a circuit simulation program. The methodology is simple, because it only requires the use of a few branch elements (resistors, capacitors, and current and voltage sources) that are connected in such a way that Kirchhoff's laws for currents and voltages are fulfilled. To perform the simulation, it is not necessary to manipulate the equations that describe the network, since the circuit simulation software does that automatically. Therefore, neither numerical nor computational aspects need to be considered. Over the past few years this method has been successfully applied to a variety of problems, including ionic transport in both membranes and electrochemical cells,[15] and nonequilibrium phenomena in colloidal suspensions.[9,13,16−18] A full account of the network model used in this work is given in ref 9, and a more general explanation of the use of the network simulation method is given in reference.[18]

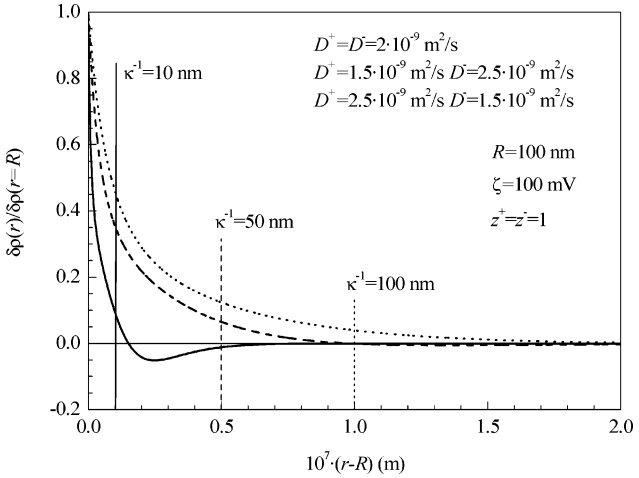

Figure 2. Perturbation of the charge density profiles, normalized to their values at the particle surface, with an applied dc electric field for the indicated κ^{-1} values. Each curve is the superposition of three curves corresponding to the three indicated combinations of diffusion coefficients. Other parameters of the simulation: univalent ions, $R = 100$ nm, and $\zeta = 100$ mV.

TABLE 1. Parameter Values Used in All the Simulations Except When Indicated Otherwise

R=100 nm	$z+ = z^- = 1$	$N = 6.022\ 10^{23}$ m^{-3}
$\zeta = 100$ mV	$\epsilon_e/\epsilon_0 = 78.54$	$\epsilon_i/\epsilon_0 = 2$
$T = 298$ K	$\eta = 0.8904\cdot10^{-4}$ poises	$\rho_f = 1000$ kg/m^3
$k_e = 0.075$ (Ω·m)$^{-1}$	$\kappa^{-1} = 10$ nm	$E = 1$ V/m

An example of the results obtained solving the resulting equation system in the steady state, that is with a dc applied electric filed, is shown in Figure 2, where the perturbations of the charge density profiles (normalized to their values at the surface of the particle) and calculated in the direction of the applied field are represented for the indicated parameter values. Each curve in the figure is actually the superposition of three curves corresponding to the results obtained for the three different combinations of diffusion coefficient values. Note that in all cases the conductivity of the electrolyte solution remains unaltered. This shows that in a dc field these values have a negligible effect on the deformation of the electric double layer and that the Debye length is, again, a good approximation of the electric double layer thickness.

Results

In what follows, we will show that the generally accepted notion that the electric double layer thickness is of the order of a few Debye lengths ceases to be valid in ac electric fields when the diffusion coefficients of the two ionic species differ from one another.

Except when indicated, the simulations were made using the parameter values shown in Table 1.

To distinguish between cases with the same conductivity but different diffusion coefficient values, we define the parameter Δ, as

$$\Delta = \frac{D^- - D^+}{D^+ + D^-} \tag{29}$$

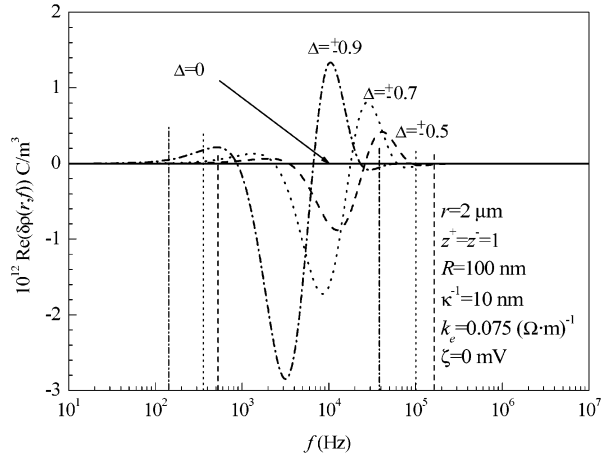

Figure 3. Real part of the perturbation of the charge density at $r = 2$ μm with an applied ac electric field for the indicated values of the parameter Δ. The remaining parameter values are given in Table 1, except for $\zeta = 0$ mV. The vertical lines represent the approximate analytical results for the minimum and maximum frequency values at which the charge densities appear and vanish: eqs 35 and 36.

which coincides for $z^+ = z^- = 1$ with the definition used in ref 19. Note that a zero value for this parameter indicates equal diffusion coefficients.

Uncharged Particles. *Dependence on the Diffusion Coefficients.* We start considering that the colloidal particles are uncharged. Exact analytical solutions for this case were recently obtained by Grosse et al.,[19] so that numerical methods are not required in order to analyze this situation. Unfortunately, there is a mistake in the presented solution for the electric potential, which is corrected in the Appendix.

In Figure 3, the real part of the charge density at $r = 2$ μm (measured in the direction of the applied field) is represented as a function of the frequency for the indicated parameter values. The figure represents, therefore, the field-induced charge density at a distance of approximately 200 Debye lengths from the particle surface. According to the usual understanding and the results presented above for the equilibrium and dc solutions, the charge density should be essentially zero at this point. Figure 3 shows that this is only the case when the diffusion coefficients of the positive and negative ions have the same value, i.e., when $\Delta = 0$. However, when these values are different, nonzero values of the charge density in a range of the frequency spectrum appear. Although these charge density values are small, they are not negligible as we will show. The most important characteristics of the curves shown in Figure 3 are as follows.

(a) The charge density increases in absolute value as the difference between the two diffusion coefficients grows.

(b) The behavior of the charge density does not change when the two diffusion coefficient values are exchanged. Thus, the curves corresponding to $D^+ < D^-$ and $D^- < D^+$ are superposed in the figure.

(c) The real part of the charge density changes its sign with frequency.

(d) The frequencies at which the charge density appears and vanishes depend on the difference between the diffusion coefficients: when the value of Δ increases, the charge density appears at lower frequencies.

These results are related to the different values of the diffusion lengths of each ionic species, and are not expected in the classical theory that does not explain them either. To analyze this seemingly anomalous behavior, we use the analytical results presented in ref 19 and corrected in this work, from which the following limiting expression for the field-induced charge density can be deduced

$$\frac{\delta\rho^*}{E\cos\theta} \rightarrow \frac{K_1\Delta^2\omega^2}{\kappa^4 D_{ef}{}^2 r^2}\left(1 + \sqrt{\frac{i\omega}{D_{ef}}}r\right)\exp\left[-\sqrt{\frac{i\omega}{D_{ef}}}(r-R)\right] \tag{30}$$

where

$$K_1 = \frac{3Ne^2R^3}{kT}\frac{\epsilon_i(2+2\kappa R+\kappa^2R^2)}{\epsilon_i(2+2\kappa R)+2\epsilon_e(2+2\kappa R+\kappa^2R^2)} \tag{31}$$

and

$$D_{\mathrm{ef}} = \frac{2D^+D^-}{D^+ + D^-} \tag{32}$$

Expression 30, which is only valid for low frequencies

$$\omega \ll \kappa^2 D_{ef} \tag{33}$$

and far from the surface of the particle

$$\kappa r \gg 1 \tag{34}$$

permits one to explain the most important features observed in Figure 3. The dependence of $\delta\rho$ on Δ^2 explains properties a and b. The sign changes of $\delta\rho'$ with frequency occur due to the imaginary part of the exponential argument in eq 30. Finally, it follows from this equation that the frequencies at which the charge density appears and vanishes can be approximated by means of

$$f_{\min} = \frac{1}{4}\frac{D_{ef}}{(r-R)^2} \tag{35}$$

$$f_{\max} = 75\frac{D_{ef}}{(r-R)^2} \tag{36}$$

The results obtained using these expressions are marked in Figure 3 with vertical lines, which are in good agreement with the numerical results in all cases.

Dependence on the Distance to the Particle and on the Particle Radius. Moreover, the arguments presented here explain other properties that can be observed performing simulations under different conditions. Thus, for spatial points closer to the particle, the charge density should appear at higher frequencies. This prediction is confirmed in Figure 4, which shows the charge density at different spatial points, all of them corresponding to many Debye lengths from the particle, as a function of frequency. Note that in this figure the charge densities are normalized to their maximum absolute values. The values obtained using expressions 35 and 36 are in good agreement with the numerical results as can be observed. Also, according to these approximate expressions, the frequency range corresponding to an appreciable charge density mainly depends on the distance to the particle surface, not to the center of the particle. This leads to a weak dependence of the charge density on R at constant r (except when R is of the order of r), as can be observed in Figure 5, where the real part of the charge density is represented as a function of the frequency for different values of the particle radius.

Dependence on the Reciprocal Debye Length. Finally, in Figure 6, we represent the real part of the charge density for different values of the reciprocal Debye length. It can be seen that, in agreement with expressions 35 and 36, the minimum and maximum frequencies corresponding to the charge density

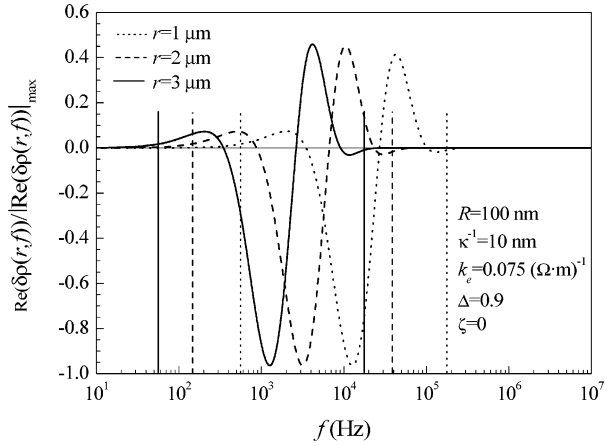

Figure 4. As in Figure 3 but for different values of r and normalized to the value at the particle surface.

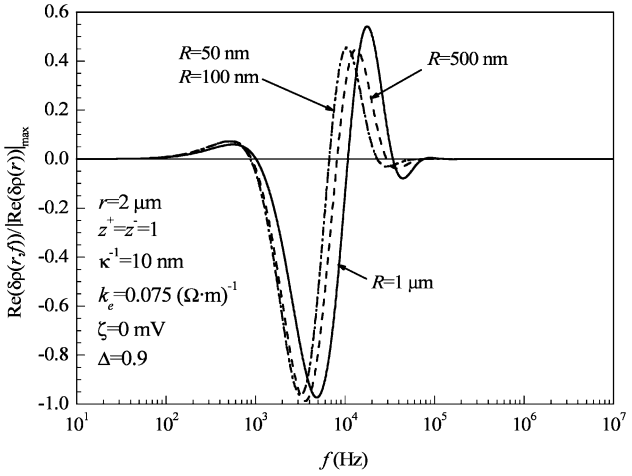

Figure 5. As in Figure 3 but for different values of R and normalized to the value at the particle surface.

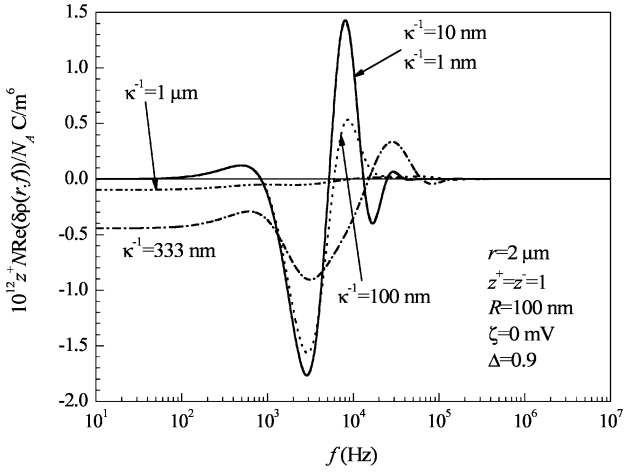

Figure 6. As in Figure 3 but for different values of κ. Note that the charge density values are multiplied by the ion concentration zN.

are practically independent of the value of κ^{-1}. Only for $\kappa^{-1} = 333$ nm and $\kappa^{-1} = 1$ μm the curves strongly change showing that the charge density persists even for very low frequencies. This behavior is to be expected since, in these cases, the values of κ^{-1} are of the order of r. This is also the reason expression 30 ceases to be valid for these cases.

Charged Particles. *Dependence on the Diffusion Coefficients.* Up to this point we only considered uncharged particles, but what happens when we consider that they are charged? To

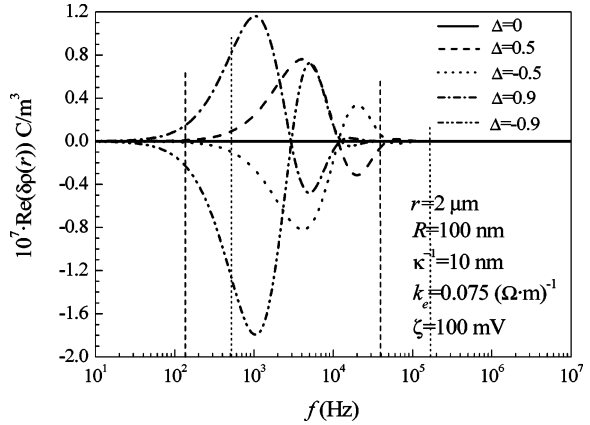

Figure 7. Real part of the perturbation of the charge density at $r = 2$ μm with an applied ac electric field for the indicated values of the parameter Δ. The remaining parameters of the simulation are given in Table 1. Vertical lines indicate the f_{min} and f_{max} frequency values given by eqs 35 and 36, respectively, for $\Delta = \pm 0.9$ (dash lines) and $\Delta = \pm 0.5$ (dot lines).

answer this question, we plotted in Figure 7 the real part of the perturbation of the charge density as a function of frequency for a particle with a ζ potential equal to 100 mV.

We first note a remarkable similarity with results corresponding to uncharged particles, Figure 3, mainly in the shape of the curves. However, there are also important differences:

(a) The perturbations of the charge density are nearly 5 orders of magnitude greater than in the case of uncharged particles.

(b) An exchange of the diffusion coefficient values now alters the results. This behavior is to be expected since the symmetry of the equilibrium ionic concentrations is lost: the system changes depending on whether the highly mobile ions are counterions or co-ions.

Dependence on the ζ Potential. The dependence of the charge density on the ζ potential can be seen in Figure 8, parts a and b. Figure 8a shows that the charge density merely grows with the ζ potential, while the value of this parameter has no appreciable influence neither on the shape nor on the location of the curves. This property is stressed in Figure 8b where the charge density has been normalized to its maximum value: the curves corresponding to the three indicated ζ potential values overlap. The second curve appearing in this figure corresponds to uncharged particles. It should be noted that the frequency ranges in which there is an appreciable charge density, coincide for charged and uncharged particles.

This leads us to the general conclusion, valid for charged and uncharged particles, that in order to guarantee electroneutrality in a system with different diffusion coefficients when ac electric fields are used, it is necessary to move to a distance from the particle surface that is larger than:

$$L > \sqrt{75\frac{D_{ef}}{f_i}} \tag{37}$$

where f_i is the lowest frequency considered in the analysis.

Dipole Coefficient. This conclusion alone is, however, insufficient since it says nothing about the influence of the charge density far from the particle on the calculated values of the dipole coefficient and the permittivity and conductivity increments. In other words, it is still necessary to determine how big are the errors that are committed when expression 7 is used at a point where there is no electroneutrality, that is when the usual assumption of electroneutrality at a few Debye lengths

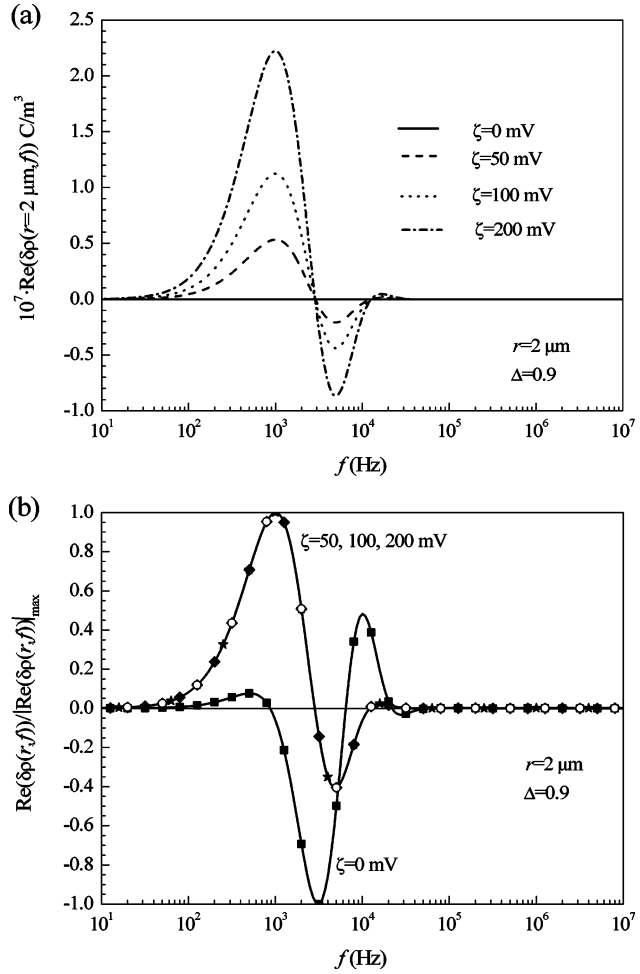

Figure 8. Real part of the perturbation of the charge density at $r = 2$ μm with an applied ac electric field, for the indicated values of the ζ potential (a). In part b, the same values are displayed, normalized to their corresponding maximum values. The remaining parameter values are given in Table 1.

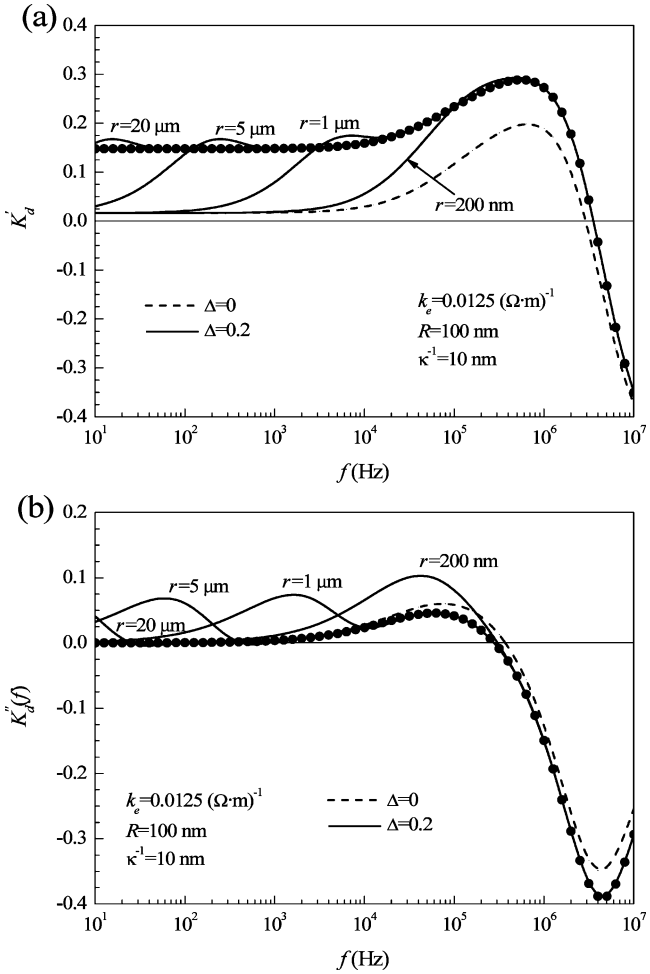

Figure 9. Real (a) and imaginary (b) parts of the dipole coefficient as functions of frequency, calculated using expression 7 at the indicated values of r (thin lines). The heavy lines with full circles correspond to the correctly calculated values, while results corresponding to identical diffusion coefficients (dash lines) are included for comparison. The parameter values are given in Table 1, except for $K_e = 0.025$ $(\Omega \cdot m)^{-1}$.

from the particle surface is used. Parts a and b of Figure 9 show the real and imaginary parts of the dipole coefficient, respectively, as functions of the frequency. Unlike previous figures that illustrated rather extreme cases, parts a and b of Figure 9 correspond to $\Delta = 0.2$, that is to a NaCl solution. The line with full circles indicates the value of the dipole coefficient, calculated using expression 7 at a point that is electroneutral for the whole range of the considered frequencies. The dashed line shows, for comparison, the results obtained for equal diffusion coefficients. The remaining curves correspond to values calculated assuming electroneutrality at the spatial points indicated in the figure.

According to the usual assumption, the electroneutrality condition should be fulfilled at all these points so that expression 7 could be used. However, the figures show that perturbations of the charge density at distances from the particle surface smaller than the diffusion length given in expression 37 lead to substantial deviations of the calculated dipole coefficient value. This is why these deviations disappear at high frequencies, when the charge density perturbations also disappear. It can also be seen that the lowest frequency boundary, below which the deviations of the calculated dipole coefficient values occur, moves to higher frequencies for points that are closer the particle. It should finally be noted that all these discrepancies in the calculation of K_d disappear when both diffusion coefficients have the same value.

Permittivity and conductivity increments. The corresponding results for the permittivity and conductivity increments calculated using expressions 4 and 5, combined with the dipole coefficient values shown in Figure 9, appear in Figure 10, parts a and b. As can be seen, the substantial deviations appearing in the calculated dipole coefficient values lead to even greater deviations of the calculated permittivity and conductivity increments. This is especially true for the permittivity increment, due to the frequency dependence of the imaginary part of the dipole coefficient curves, that even change sign at low frequencies. It should be noted that both Figure 9a and 10b could lead to the wrong conclusion that, for low frequencies, all the thin lines coincide with the dashed curve. This is not true in general: for higher values of the Δ parameter, the thin lines converge to a limit that differs from the dashed curve.

We finally note that Figures 9 and 10 should not be interpreted in the sense that all numerical calculations on NaCl suspensions, performed assuming electroneutrality at a few Debye lengths from the particle, should lead to the huge deviations shown in these figures. When the dipole coefficient is numerically calculated at a distance of a few Debye lengths from the particle, the assumption is made that the system is electroneutral at this and at all greater distances. Therefore, it is also postulated that the charge density far from the particle does not exist. This means that two errors are made: the first

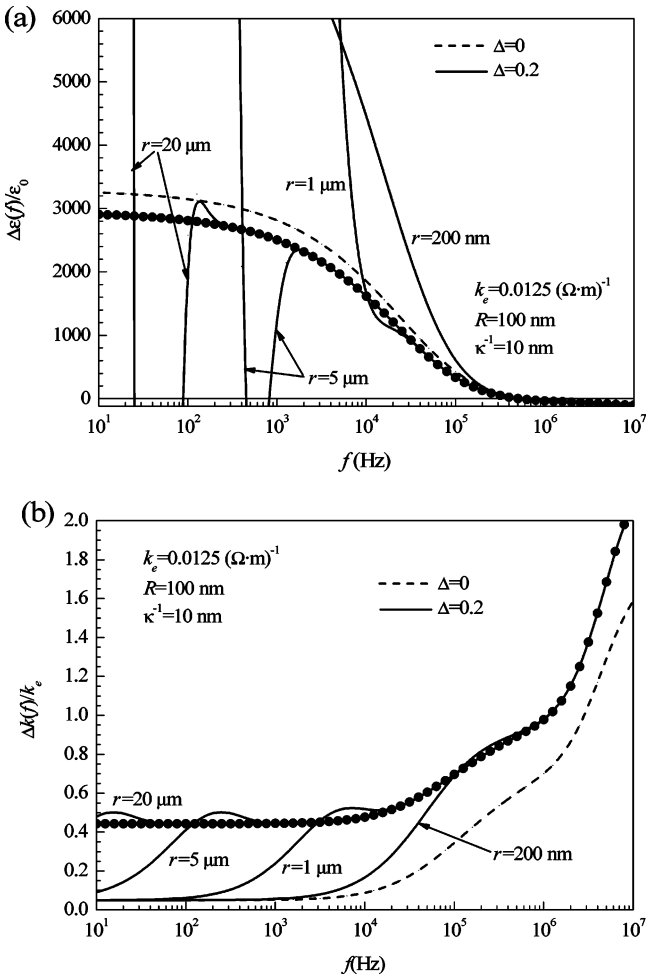

Figure 10. Permittivity (a) and conductivity (b) increments as functions of frequency, calculated using expressions 4, 5, and 7 at the indicated values of r (thin lines). The heavy lines with full circles correspond to the correctly calculated values, while results corresponding to identical diffusion coefficients (dash lines) are included for comparison. The parameter values are given in Table 1, except for $K_e = 0.025$ $(\Omega\cdot m)^{-1}$.

in the calculation of the potential, without considering the influence of the charge density far from the particle. The second in the calculation of the dipole coefficient at a point that is not electroneutral in reality, but becomes electroneutral by hypothesis. On the contrary, Figures 9 and 10 show results obtained when the potential is correctly calculated, while the only error is in the calculation of the dipole coefficient, by using eq 7 at a point where it is not valid. It appears that this way of doing amplifies the deviations, while the above-mentioned errors mostly compensate each other when electroneutrality is imposed upon the system.

Conclusions

The main conclusions of this work can be summarized as follows.

•Electroneutrality in the electrolyte solution is always attained at a few Debye lengths from the particle surface for dc electric fields. However, for ac fields, this is only true when the diffusion coefficients of the two ionic species are identical.

•In the general case, i.e., when the diffusion coefficient values differ from one another and for ac fields, electroneutrality is attained at a much larger distance from the particle surface that is determined by the characteristic diffusion lengths of the ions. It is proportional, therefore, to the square root of the effective diffusion coefficient divided by the electric field frequency.

•While the value of the field-induced charge density increases with the ζ potential, numerical results for charged particles show that electroneutrality is attained at a distance that does not depend on the ζ potential and coincides, furthermore, with the corresponding distance for uncharged particles, eq 37.

•Although the charge densities far from the particle are usually very weak, they strongly contribute to the dipole coefficient value and, therefore, to the calculated permittivity and conductivity increments.

•The errors that would be committed if these charge densities were ignored, assuming local electroneutrality and determining the dipole coefficient at a few Debye lengths from the particle surface, can be very important.

•Even when the dipole coefficient is determined at a point distant many Debye lengths from the particle surface, it should only be used to calculate the permittivity and conductivity increments for frequencies higher than a limiting value given in expression 37.

Acknowledgment. Financial support by Ministerio de Ciencia y Tecnología, Spain, under project BFM2003-4856, and by the Consejo de Investigaciones de la Universidad Nacional de Tucumán, Agencia Nacional de Promoción Científica y Tecnológica, and Consejo Nacional de Investigaciones Científicas y Técnicas, Argentina, is gratefully acknowledged.

Appendix

The expression for the electric potential presented in ref 19, eq 4, contains a mistake. The corrected result is

$$\frac{\Phi}{E\cos\theta} = \left(\frac{K_d R^3}{r^2} - r\right) + \frac{kT\kappa^2}{e}\left[\frac{\beta K_u}{\rho^2}H(\rho,r)e^{\rho(R-r)} + \frac{K_v}{\sigma^2}H(\sigma,r)e^{\sigma(R-r)}\right] \quad (38)$$

Because of this correction, the expressions for the coefficients determined from the boundary conditions, change to

$$K_d = \{(\epsilon_i - \epsilon_e)(1-\alpha\beta)\rho^2\sigma^2 G_1 G_2 R - \epsilon_i\kappa^2[\rho^2 G_1(G_2 R - H_2) - \alpha\beta\sigma^2 G_2(G_1 R - H_1)]\}/\{(\epsilon_i + 2\epsilon_e)(1-\alpha\beta)\rho^2\sigma^2 G_1 G_2 R - \epsilon_i\kappa^2[\rho^2 G_1(G_2 R + 2H_2) - \alpha\beta\sigma^2 G_2(G_1 R + 2H_1)]\} \quad (39)$$

$$K_u = \{3\epsilon_i e\alpha\rho^2\sigma^2 G_2 R/(kT)\}/\{(\epsilon_i + 2\epsilon_e)(1-\alpha\beta)\rho^2\sigma^2 G_1 G_2 R - \epsilon_i\kappa^2[\rho^2 G_1(G_2 R + 2H_2) - \alpha\beta\sigma^2 G_2(G_1 R + 2H_1)]\} \quad (40)$$

$$K_v = \{-3\epsilon_i e\rho^2\sigma^2 G_1 R/(kT)\}/\{(\epsilon_i + 2\epsilon_e)(1-\alpha\beta)\rho^2\sigma^2 G_1 G_2 R - \epsilon_i\kappa^2[\rho^2 G_1(G_2 R + 2H_2) - \alpha\beta\sigma^2 G_2(G_1 R + 2H_1)]\} \quad (41)$$

where the different symbols are defined in ref 19.

Fortunately, these corrected results have no bearing on the final expression for the dipole coefficient K_d, so that all the conclusions in ref 19 related to the dielectric properties of the system remain unaltered. However, the final expressions for the ion concentrations and, therefore, for the field-induced charge density do change.

References and Notes

(1) Dukhin, S. S.; Shilov, V. N. *Dielectric Phenomena and the Double Layer in Disperse Systems and Polyelectrolytes*; Wiley: NewYork, 1974.

(2) Lyklema, J. *Fundamentals of Interface and Colloid Science*; Academic Press: New York, 1995; Vol. II, Chapter 4.
(3) O'Brien, R. W. *Adv. Colloid Interface Sci.* **1982**, *16*, 281.
(4) Fixman, M. *J. Chem. Phys.* **1983**, *78*, 1483.
(5) Vogel, E.; Pauly, H. *J. Chem. Phys.* **1988**, *89*, 3830.
(6) Grosse, C.; Shilov, V. N. *J. Phys. Chem.* **1996**, *100*, 1771.
(7) DeLacey, E. H. B.; White, L. R. *J. Chem. Soc., Faraday Trans. 2*, **1981**, *77*, 2007.
(8) Mangelsdorf, C. S.; White, L. R. *J. Chem. Soc., Faraday Trans.* **1992**, *88*, 3567.
(9) López-García, J. J.; Horno, J.; González-Caballero, F.; Grosse, C.; Delgado, A. V. *J. Colloid Interface Sci.* **2000**, *228*, 95.
(10) Loeb, A. L.; Wiersema, P. H.; Overbeek, J. Th. G. *The Electrical Double Layer around a Spherical Colloid Particle*; MIT Press: Cambridge, MA, 1961.
(11) White, L. R. *J. Chem. Soc., Faraday Trans. 2* **1977**, *73*, 577.
(12) Chen, I. *Langmuir* **1996**, *12*, 3437.
(13) López-García, J. J.; Moya, A. A.; Horno, J.; Delgado, A.; González-Caballero, F. *J. Colloid Interface Sci.* **1996**, *183*, 124.
(14) Quian, Y.; Deng, H.; Yang, G. *Dianhuaxue* **1997**, *3*, 244.
(15) Moya, A. A.; Horno, J. *J. Phys. Chem. B* **1999**, *103*, 10791.
(16) López-García, J. J.; Grosse, C.; Horno, J. *J. Colloid Interface Sci.* **2003**, *265*, 327.
(17) López-García, J. J.; Grosse, C.; Horno, J. *J. Colloid Interface Sci.* **2003**, *265*, 341.
(18) López-García, J. J.; Horno, J. In *Network Simulation Method*; Horno, J., Ed.; Research Signpost: Trivandrum, India, 2002.
(19) Grosse, C.; López-García, J. J.; Horno, J. *J. Phys. Chem. B* **2004**, *108*, 8397.